Significant electron-phonon coupling in nanographene confined in single-walled carbon nanotubes due to the large amplitude of radial breathinglike vibrations

Bingze Wu,[1] Mingfeng Zhu,[2] Chunguang Zhai,[1] Yaping Zhao,[1] Yexuan Meng,[2] Jiajun Dong,[1] Xuan Li,[3] Ran Liu,[1] Kunpeng Tang,[3] Lei Shi,[3,*] Bertil Sundqvist,[4] and Mingguang Yao[1,†]

[1]*State Key Laboratory of Superhard Materials, College of Physics, Jilin University, Changchun 130012, China*

[2]*College of Physics, Jilin University, Changchun 130012, China*

[3]*State Key Laboratory of Optoelectronic Materials and Technologies, Guangdong Basic Research Center of Excellence for Functional Molecular Engineering, Nanotechnology Research Center, School of Materials Science and Engineering, Sun Yat-sen University, Guangzhou 510275, China*

[4]*Department of Physics, Umeå University, SE-90187 Umeå, Sweden*

(Received 13 July 2023; revised 8 April 2024; accepted 16 April 2024; published 6 May 2024)

One-dimensional (1D) van der Waals heterostructures (vdWHs) exhibit many properties, but many of these are difficult to understand because of their complicated structures and host-guest couplings that remain challenging to understand. Here, we observe a significant electron-phonon coupling (EPC) in 1D armchair graphene nanoribbons (AGNRs) confined in single-walled carbon nanotubes (SWNTs) via resonance Raman spectroscopy combined with theoretical calculation. A strong coupling between radial breathinglike mode (RBLM) phonons and the host nanotubes occurs due to the large vibration amplitude of RBLMs of the guest AGNRs. This results in unique deformation potential interactions in the heterostructure, contributing to the observed EPC enhancement. The EPC could be further modulated and strengthened by high pressure through tuning the RBLM-nanotube interactions. In this paper, we discover a mechanism governing the EPC in vdWHs and pave the way for manipulating the host-guest EPC for further control of the physical properties and potential device applications.

DOI: 10.1103/PhysRevB.109.195413

I. INTRODUCTION

Functional heterostructures play an increasingly essential role in the development of modern electronic and optoelectronic devices [1–4]. The integration of different materials may induce a wide range of properties, including high electron mobility, high efficiency light emission, and superconductivity [3–6]. Van der Waals (vdW) heterostructures (vdWHs) can be designed by physically assembling building blocks through weak vdW interactions, showing no requirements from lattice matching between building blocks, processing compatibility during preparation, and even dimensionality [7,8]. This stimulates great enthusiasm in the study of vdWHs with various structural dimensionalities, including two-dimensional (2D), one-dimensional (1D), and mixed-dimensional [9–11], displaying enormous prospects of properties and potential applications.

The properties of vdWHs strongly depend on the interactions of the composed building blocks. To achieve the goal of more is different [12], understanding and tuning the interactions in vdW systems is thus very important for obtaining further properties. For 2D vdWHs, interlayer interactions have been extensively studied, and properties like correlated insulating states and superconducting phases due to the strong interlayer coupling in moiré superlattice [13–15] as well as interlayer excitons with lifetimes larger than intralayer excitons due to the spatial charge separation have been reported [16–18]. Recently, it was also revealed that the interlayer electron-phonon interaction in transition metal dichalcogenide/hexagonal boron nitride (hBN) heterostructures originates from a dipole-dipole interaction between adjacent layers, which is related to the out-of-plane vibrations of the 2D lattice and could be enhanced by application of high pressure [19–22].

As material dimensionality further decreases to one dimension, structures and properties significantly different from those of the corresponding higher-dimensionality counterparts are often observed. For example, long carbon chains and tellurium atomic chains have been stabilized inside carbon nanotubes [23,24]; very small single-wall carbon nanotubes (SWNTs) confined in a zeolite matrix exhibit superconductivity with a T_c of 15 K [25]. Note that such 1D structures usually are not stable in an isolated state at ambient conditions but become stable in a confining environment due to host-guest interactions. Moreover, 1D structures may exhibit vibration modes that are distinct from those of their 2D/three-dimensional (3D) counterparts [26–28], which could interact with the host and result in complex and intricate guest-host coupling effects in 1D vdWH systems. Up to now, host-guest charge transfer effect and spatial nanoconfinement effect are usually used to explain the structures and properties observed in 1D vdWHs [29–32]. However, many of the resulting phenomena are still not well understood or even under debate. Some examples are the configurations of

*shilei26@mail.sysu.edu.cn
†yaomg@jlu.edu.cn

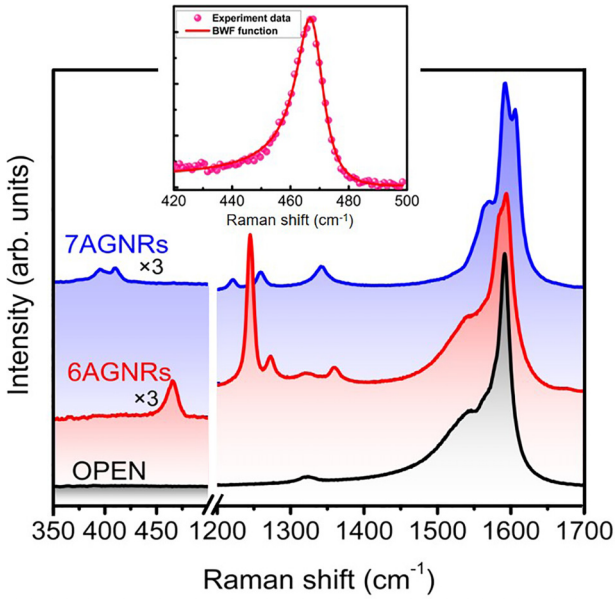

FIG. 1. The Raman spectra of opened single-walled carbon nanotubes (SWNTs; black), 6 armchair graphene nanoribbons (AGNRs)@SWNTs (red), and 7 AGNRs@SWNTs (blue). The excitation wavelengths used are 633 nm/514 nm, 633 nm, and 514 nm, respectively. The inset shows the radial breathinglike mode (RBLM) of 6 AGNRs fitted by the Breit-Wigner-Fano (BWF) function (see text).

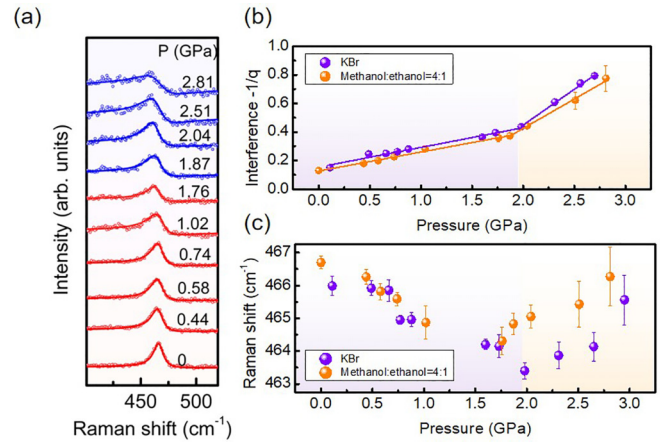

FIG. 2. The Raman spectra of 6 armchair graphene nanoribbons (AGNRs) under pressure under excitation by a 633 nm laser. (a) The radial breathinglike mode (RBLM) peak of 6 AGNRs under different pressures. (b) The dependence of the Fano resonance factor on pressure for the RBLM of 6 AGNRs with two kinds of pressure transmitting medium (PTM). To exclude the possibility of the methanol and ethanol molecules penetrating carbon nanotubes and affecting the transition of nanoribbons, we carried out a comparison experiment by using solid KBr as PTM. (c) The dependence of the Raman shift of the RBLM of 6 AGNRs on pressure.

confined 1D structures that are quite different from their bulk counterparts and stabilized by complex host-guest interactions [33–36], the giant Raman intensity enhancement of confined 1D structures in carbon nanotubes [37,38], and the anomalous Raman frequency response of atomic chains at ambient and high pressure [24,39–42]. Clarifying the interactions between the host and guest components and the mechanism of coupling effects in 1D vdWHs is thus urgently required and important to further understand such properties and develop potential applications of 1D vdWHs in the future.

Here, we report an interaction mechanism governing the electron-phonon coupling (EPC) effects in vdWHs, that is, armchair graphene nanoribbons (AGNRs) confined inside SWNTs (AGNRs@SWNTs). The significant EPC effect in guest graphene nanoribbons is related to deformation potential scattering in this 1D vdWH, which is different from the Fröhlich coupling in 2D and mixed-dimensional vdWHs. It is further revealed that the large vibration amplitude of the radial breathinglike mode (RBLM) of the guest AGNR generates unique interactions with host nanotubes, leading to a significant deformation potential scattering. Accordingly, the EPC was further modulated and strengthened by high pressure through tuning the RBLM-nanotube interactions.

II. RESULTS and DISCUSSION

AGNR@SWNT samples were synthesized by a method reported elsewhere [43], in which two kinds of well-defined AGNRs, 6 AGNRs and 7 AGNRs, were obtained (detailed descriptions are shown in the Supplemental Material [44]). As shown in Fig. 1, the Raman spectra of AGNRs@SWNTs show obviously resonant features depending on the excitation laser wavelengths. Here, 6 AGNRs confined in metallic SWNTs are resonant with a wavelength of 633 nm, while 7 AGNRs in semiconducting SWNTs are resonant at 514 nm. Note that the low-frequency RBLM, which is absent in 2D graphene but present in nanoribbons due to the dimension decrease, reflects the transverse breathing vibration of the AGNRs and scales with the inverse square root of the nanoribbon width. As we can see from the inset of Fig. 1, the RBLM of 6 AGNRs shows an asymmetric line shape with a phonon frequency at 467 cm^{-1}, which agrees well with the theoretically calculated frequency (465 cm^{-1}) for the 6 AGNRs [28]. In contrast, the RBLM of 7 AGNRs displays two peaks under excitation of the 514 nm laser, located at 397 and 411 cm^{-1}, respectively, which is different from the theory (402 cm^{-1}) and should be due to a splitting because of the radial curvature of nanoribbons confined inside carbon nanotubes. This will be further discussed in connection with our high-pressure experiments.

It should be noted that the asymmetric line shape of the RBLM of 6 AGNRs confined in metallic SWNTs (mSWNTs) is different from the symmetric RBLMs observed in narrow AGNRs on Au/mica substrate, for example, 9 AGNRs, which have properties like those of 6 AGNRs [49,50]. Moreover, the asymmetric line shape of the RBLM of 6 AGNRs confined in mSWNTs cannot be fitted by Lorentz functions because of the observed antiresonance dip toward the higher-energy side, which is a typical feature of Fano resonance [51,52], as shown in Figs. 2(a) and S1(a) in the Supplemental Material [44]. Indeed, it can be well fitted by the asymmetric Breit-Wigner-Fano (BWF) function which is written as $I(\omega) = I_0 \frac{[1+2(\omega-\omega_0)/q\Gamma]^2}{1+[2(\omega-\omega_0)/\Gamma]^2}$, where ω_0, I_0, and Γ are fitting parameters for the central frequency, the intensity, and the broadening factor, respectively, and $-1/q$ is a factor that measures the asymmetry of the band [53]. Generally speaking, the emergence of a BWF

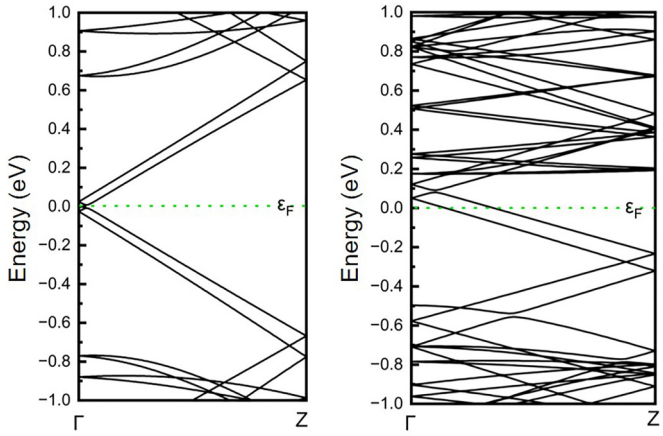

FIG. 3. The band structure of (a) unfilled (15,3) single-walled carbon nanotubes (SWNTs) and (b) hybrid 6 armchair graphene nanoribbons (AGNRs) @(15,3) SWNTs. The dotted lines represent the Fermi levels.

line shape always originates from a Fano resonance, which is the result of the interference of a discrete phonon spectrum and a continuum exciton spectrum [it is electronic Raman scattering (ERS) for a Raman spectrum], and the asymmetry factor $-1/q$ describes the degree of the interference [54–59]. In our experiments, the positive Fano factor $-1/q$ in the BWF line shape of the RBLM indicates that the ERS features appear at a frequency region lower than the RBLM, indicating the presence of low-energy electron-hole pairs with energies lower than the RBLM of 6 AGNRs in this system [60]. These should not come from intrinsic interband transitions of the semiconducting 6 AGNRs (band gap 1.83 eV).

To understand how the EPC occurs in 6 AGNRs confined in mSWNTs, we performed *ab initio* electronic band structure calculations on 6 AGNRs@(15,3)SWNT and compared with pristine (15,3)SWNT, which is the nanotube closest to our experimental ones [61] (calculation details are given in the Supplemental Material [44]). The results are shown in Fig. 3. The electronic states of 6 AGNRs and the nanotube are hybridized, rather than a simple superposition of each constituent as observed in most previous confinement systems [62,63], indicating a nonnegligible interaction between the graphene nanoribbons and the nanotubes. Note that 6 AGNRs@(15,3)SWNT are metallic with no gap and that the lowest conduction band and the highest valence band are both from the metallic nanotube, giving the possibility for the generation of low-energy electron-hole pairs created across the linear electronic subbands near the Dirac point of the host SWNTs. Our Raman measurements indeed show that an unusual intensity enhancement for RBMs of SWNTs occurs under excitation of a 633 nm laser (Fig. S3 in the Supplemental Material [44]). Such a significant RBM enhancement could be ascribed to the emergence of low-frequency ERS near the RBM position according to previous literature [60,64]. A transition energy ∼1.94 eV of the host mSWNTs could be observed in the wavelength-dependent Raman spectroscopy [43], which could result in ERS with low frequency. The ERS resonating with the low-energy electron-hole pairs couples with the RBLM phonons of the 6 AGNRs, giving a significant EPC. In contrast, no visible EPC was observed in the 7 AGNRs confined in semiconducting SWNTs, probably due to the absence of low-energy electron-hole pairs in the semiconducting nanotubes [65].

To further support our interpretation and to achieve a modulation of the EPC, high pressure has been applied to tune the host-guest interaction strength (experimental details are given in the Supplemental Material [44]). *In situ* high-pressure Raman measurements showed that the RBLM peak of 6 AGNRs always shows a Fano line shape during compression, and the antiresonance dip character becomes more obvious upon compression, as shown in Figs. 2(a) and S1(a) in the Supplemental Material [44]. By fitting the BWF function to the recorded RBLM peaks, we obtained the pressure dependence of the interference factor $-1/q$ upon compression. A sudden increase in the pressure slope ∼1.8 GPa was observed at the well-known ovalization transformation of the nanotubes [66–68], indicating a gradual enhancement of the strength of the EPC above this pressure, as shown in Figs. 2(b) and S5(a) in the Supplemental Material [44]. In addition to the Fano interference factor, the frequency of the RBLM of 6 AGNRs also shows an interesting pressure evolution upon compression, displaying first a redshift and then a blueshift as pressure increases [Fig. 2(c)]. Note the phonon frequency obtained by fitting a BWF function does not coincide with the position of the maximum intensity of the broad Fano resonance function [59]. Since the RBLM frequency is related to the width of the nanoribbons, such a pressure evolution suggests that the confined nanoribbons first become wider and then narrower. The widening of nanoribbons upon compression can be understood by their positive Poisson's ratios [69]. As pressure increases further and the nanotube cross-sections change from circular to elliptical ∼1.8 GPa, the interactions between nanoribbon and tube wall are enhanced, causing the reduction of its width. This transition thus affects the width of 6 AGNRs and gives an enhancement of the EPC, indicating that the width variation of 6 AGNRs significantly affects the host-guest interaction. This, on the other hand, provides additional evidence to rule out a phonon confinement effect which could be an alternative reason for the observed asymmetric Raman line shape in 6 AGNRs@mSWNTs.

In contrast, the high-pressure Raman spectra recorded from 7 AGNRs confined in semiconducting SWNTs (sSWNTs) show that the RBLM peaks of 7 AGNRs can be well fitted by using Lorenzian functions, and the results are shown in Figs. 4(a) and S1(b) in the Supplemental Material [44]. Note that no visible spectroscopic characteristic for EPC was observed upon compression. It can be seen that the right RBLM peak shows a frequency downshift and rapid intensity attenuation and then vanishes as pressure increases, while the left peak shows a slow downshift in frequency and then a transition in frequency from decrease to increase at ∼2 GPa (Figs. 4(b) and S6 in the Supplemental Material [44], dependence of the Raman linewidths are shown in Fig. S5(b) in the Supplemental Material [44]). This corresponds to a change from a double to a single RBLM peak, indicating an uncurling or flattening process of 7 AGNRs due to the ovalization of nanotube. The comparison experiments further demonstrate that the host nanotubes are critical for EPC enhancement of the guest graphene nanoribbons and that the

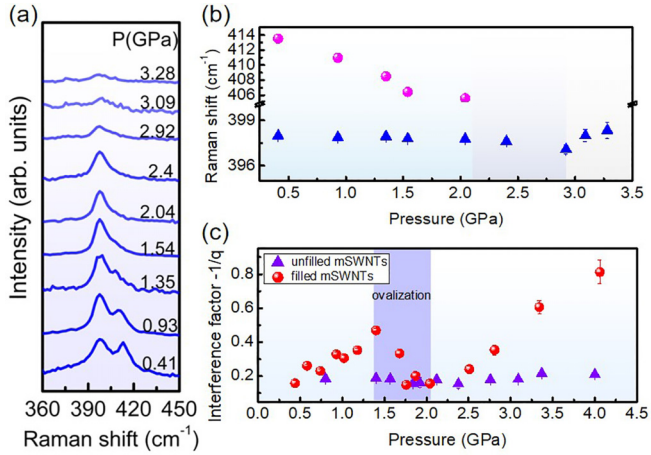

FIG. 4. (a) The radial breathinglike mode (RBLM) peak of 7 armchair graphene nanoribbons (AGNRs) confined in semiconducting single-walled carbon nanotubes (SWNTs) at different pressures under excitation by a 514 nm laser. (b) The dependence of the RBLM peak positions of 7 AGNRs on pressure. (c) The variation of the interference factor $-1/q$ of the G^- band for 6 AGNRs filled and for unfilled metallic SWNTs under pressure under excitation by a 633 nm laser.

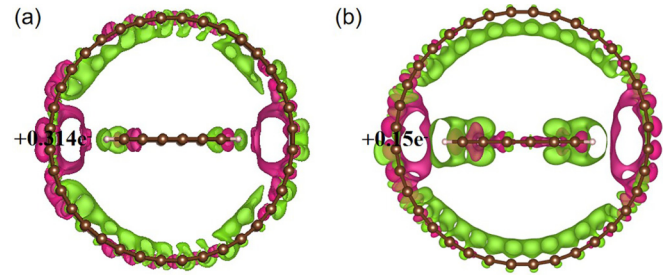

FIG. 5. Charge differential density for (a) the narrowest state and (b) widest state of 6 armchair graphene nanoribbons (AGNRs) during radial breathing. The pink and green areas represent the increasing and decreasing of charge density, respectively.

metallic host tubes contribute significantly to the presence of EPC.

The graphene nanoribbons confined inside metallic SWNTs also modify the pressure evolutions of the host. As shown in Figs. 4(c) and S4 in the Supplemental Material [44], the variation of the BWF interference factor for the G^- band of the mSWNTs with pressure displays a strong anomaly in the transition region ∼2 GPa. This is quite different from the same unfilled mSWNTs, for which the BWF interference factor of the G^- band is almost constant as pressure increases. All high-pressure experiments thus show that, at ∼2 GPa, the pressure dependence of RBLMs of both 6 AGNRs and 7 AGNRs as well as the interference factors for 6 AGNRs and the host metallic nanotubes exhibit obvious anomalies. Such simultaneous transitions of guest 6 AGNRs and host mSWNTs indicate that the change in EPC is related to the host-guest interaction variation. As mentioned above, the SWNTs used here should undergo a transition from circular to ellipsoidal cross-sections at ∼2 GPa, where we observed a transition in the width of 6 AGNRs from an increase to a decrease with increasing pressure. This indicates a significant enhancement of the host-guest interaction, accompanied by an obvious enhancement of the EPC strength in the 6 AGNRs. These results confirm that the EPC observed should be related to the coupling between the RBLM of the guest AGNRs and the host mSWNTs.

It is worth noting that the interlayer EPC in 2D vdWHs has been attributed to Fröhlich coupling, which arises due to the dipole-dipole interaction between out-of-plane phonon and excitons in adjacent layers [20]. However, such a coupling should not be responsible for the EPC in our 1D vdWHs because the RBLM of AGNRs is a transverse optical (TO) mode which can hardly generate dipole coupling. We discovered that the host-guest EPC in AGNRs@SWNTs vdWHs is primarily caused by deformation potential scattering, which contributes to the EPC of optical modes in nonpolar materials [70–75]. To further explore the origin of deformation potential scattering in our 1D vdWHs, we carried out a vibration analysis for AGNRs@SWNTs vdWHs (calculation details are given in the Supplemental Material [44]) [48]. Considering that the deformation potential scattering is mainly related with the amplitude of radial breathing vibrations of the guest and host, we calculated the atomic displacements connected with the RBLM for 6 AGNRs and the RBM for the SWNT. Our calculations show that the displacement induced by the RBLM reaches a maximum of 0.32 Å, which is much larger than that of the radial breathing vibration of the SWNT (∼ 0.16 Å). Such a giant amplitude of the RBLM of the guest 6 AGNRs could induce a significant deformation potential scattering in this 1D vdWH system.

To investigate how the large-amplitude RBLM affects the host-guest EPC in an AGNR@SWNT system, we calculate the charge differential density for optimized 6 AGNRs@(18,0)SWNT (Fig. S7 in the Supplemental Material [44]), which is a 1D vdWH model close to our experiment (calculation details are given in the Supplemental Material [44]). We observed substantial electron redistribution for the host SWNT, that is, electron accumulation on the nanotube wall in the regions near the two edges of AGNR. Consequently, in-plane electrons are pushed from the nanoribbon edges toward its center due to charge repulsion. Further calculations for charge differential density and Bader charge analysis show that the charge oscillation on a graphene nanoribbon is changed obviously as the RBLM vibrates [Figs. 5(a) and 5(b)], accompanying the variation of the electron accumulation on the nanotube wall. Notably, the maximum electron accumulation on the tube wall occurred at the narrowest state of the 6 AGNRs during radial breathing, which was twice as large as that at the widest state of the 6 AGNRs. These findings suggest that the host-guest EPC in 1D vdWHs is related to deformation potential coupling, originating from significant RBLM vibrations of the guest. This coupling mechanism differs from the indirect Fröhlich coupling observed in 2D systems.

We calculated deformation potential coefficient to further explore the origin of host-guest EPC enhancement in our 1D vdWHs. For this purpose, we employed density functional theory (DFT) to calculate the variation of the conduction band minimum (CBM) and valence band maximum (VBM) of the

band structure for an AGNR@SWNT under strain applied along the radial direction of nanoribbon. This allows us to extract the deformation potential coefficient caused by RBLM [76]. Note that the 6 AGNRs@(18,0)SWNT model was used again for the simulation because the host nanotube diameter is close to that of our experiment. Both the CBM and VBM show the same slope with the variation of strain (Fig. S9 and Table S1 in the Supplemental Material [44]), giving a deformation potential coefficient of 11.3 eV, larger than the value of isolated 6 AGNRs (10.3 eV). This indicates that the introducing of host SWNT enhances the deformation potential scattering for RBLM of the confined 6 AGNRs. To further understand the effect of charge accumulation of host tube on EPC enhancement, we put two Na atoms at two opposite sides of 6 AGNRs (no bonding between Na and nanoribbon) to simulate the conditions for 6 AGNRs confined within the SWNT. The charge differential density calculations show that an in-plane charge change occurs in the 6 AGNRs, like that observed in the 6 AGNRs confined in the SWNT (Fig. S8 in the Supplemental Material [44]). In this case, the deformation potential coefficient of the system increases significantly to 16.85 eV, indicating a substantial EPC enhancement due to the presence of the charge accumulation surrounding the nanoribbons. The results further confirm that the host-guest deformation potential scattering arises from the interaction between charge accumulation on the host nanotube wall and the large-amplitude vibration of RBLM, serving as the basis for the host-guest EPC observed in our experiments. This presents a unique type of host-guest interaction in 1D vdWHs, which is different from that previously reported for 2D vdWHs.

We also noticed that a splitting of the CH in-plane bending (CH-ipb) mode at 1246 cm^{-1} occurs ~2 GPa during compression, a peak occurs at 1245 cm^{-1}, and its intensity increases as pressure increases (Fig. S10 in the Supplemental Material [44]). In a previous study, the splitting of CH-ipb in pentacene, which can be regarded as a building block of AGNRs, has been ascribed to Davydov splitting originating from the interaction between CH-ipb and the gate field or neighboring molecules [77–82]. In our 6 AGNRs, the splitting of CH-ipb under pressure might be due to the increased interaction between the charge accumulation (which generates built-in electric field) and the in-plane vibration of the guest 6 AGNRs. Moreover, the splitting of CH-ipb occurs at the pressure where host-guest EPC enhanced suddenly, giving further support that the charge accumulation of host tube play an essential role in EPC. Note that EPC can significantly influence the physical properties of materials, such as the electric and thermal transport, the light-matter interaction, and the superconductivity [83–85]. The manipulation of EPC, for example, by application of high pressure demonstrated here, should be beneficial to engineer 1D vdWHs with a potential for electronic and optoelectronic applications.

III. CONCLUSION

In summary, we discovered that deformation potential scattering dominantly contributes to the EPC effects observed in the confined graphene nanoribbon, which is a mechanism governing the EPC in vdWHs. The 1D graphene nanoribbons exhibit RBLMs which induce significant host-guest interaction due to their very large amplitudes compared with the RBM of the host tube. This results in a strong coupling between RBLM phonons and host nanotubes. The EPC can be further enhanced and modulated by modifying the host-guest interactions with high pressure. In this paper, we also emphasize the importance of dimensionality-decrease-induced vibration modes of the 1D structure on the coupling in 1D vdWHs, which could be extended to other 1D vdW systems, and give insights into the related puzzling phenomena in previous studies.

ACKNOWLEDGMENTS

This paper was supported financially by the National Natural Science Foundation of China (Grants No. 52225203, No. 12274170, No. 12104175, and No. 12304017) and Guangzhou Basic and Applied Basic Research Foundation (Grant No. 202201011790), the Program of China Postdoctoral Science Foundation (2023M741351).

[1] Y. Liu, N. O. Weiss, X. D. Duan, H. C. Cheng, Y. Huang, and X. F. Duan, Van der Waals heterostructures and devices, Nat. Rev. Mater. **1**, 16042 (2016).

[2] K. S. Novoselov, A. Mishchenko, A. Carvalho, and A. H. C. Neto, 2D materials and van der Waals heterostructures, Science **353**, aac9439 (2016).

[3] A. S. Mayorov, R. V. Gorbachev, S. V. Morozov, L. Britnell, R. Jalil, L. A. Ponomarenko, P. Blake, K. S. Novoselov, K. Watanabe, T. Taniguchi *et al.*, Micrometer-scale ballistic transport in encapsulated graphene at room temperature, Nano Lett. **11**, 2396 (2011).

[4] J. S. Ross, P. Klement, A. M. Jones, N. J. Ghimire, J. Q. Yan, D. G. Mandrus, T. Taniguchi, K. Watanabe, K. Kitamura, W. Yao *et al.*, Electrically tunable excitonic light-emitting diodes based on monolayer WSe_2 $p-n$ junctions, Nat. Nanotechnol. **9**, 268 (2014).

[5] S. Choi, S. Johnston, W. J. Jang, K. Koepernik, K. Nakatsukasa, J. M. Ok, H. J. Lee, H. W. Choi, A. T. Lee, A. Akbari *et al.*, Correlation of Fe-Based superconductivity and electron-phonon coupling in an FeAs/oxide heterostructure, Phys. Rev. Lett. **119**, 107003 (2017).

[6] H. Yang, Y. Y. Li, T. T. Liu, D. D. Guan, S. Y. Wang, H. Zheng, C. H. Liu, L. Fu, and J. F. Jia, Multiple in-gap states induced by topological surface states in the superconducting topological crystalline insulator heterostructure $Sn_{1-x}Pb_xTe-Pb$, Phys. Rev. Lett. **125**, 136802 (2020).

[7] Y. Liu, Y. Huang, and X. F. Duan, Van der Waals integration before and beyond two-dimensional materials, Nature (London) **567**, 323 (2019).

[8] C. R. Dean, A. F. Young, I. Meric, C. Lee, L. Wang, S. Sorgenfrei, K. Watanabe, T. Taniguchi, P. Kim, K. L. Shepard *et al.*, Boron nitride substrates for high-quality graphene electronics, Nat. Nanotechnol. **5**, 722 (2010).

[9] S. Cambre, M. Liu, D. Levshov, K. Otsuka, S. Maruyama, and R. Xiang, Nanotube-based 1D heterostructures coupled by van der Waals forces, Small **17**, 2102585 (2021).

[10] R. Xiang, T. Inoue, Y. J. Zheng, A. Kumamoto, Y. Qian, Y. Sato, M. Liu, D. M. Tang, D. Gokhale, J. Guo *et al.*, One-dimensional van der Waals heterostructures, Science **367**, 537 (2020).

[11] D. Jariwala, T. J. Marks, and M. C. Hersam, Mixed-dimensional van der Waals heterostructures, Nat. Mater. **16**, 170 (2017).

[12] P. W. Anderson, More is different, Science **177**, 393 (1972).

[13] R. Bistritzer and A. H. MacDonald, Moiré bands in twisted double-layer graphene, Proc. Natl. Acad. Sci. U.S.A. **108**, 12233 (2011).

[14] Y. Cao, V. Fatemi, A. Demir, S. Fang, S. L. Tomarken, J. Y. Luo, J. D. Sanchez-Yamagishi, K. Watanabe, T. Taniguchi, E. Kaxiras *et al.*, Correlated insulator behaviour at half-filling in magic-angle graphene superlattices, Nature (London) **556**, 80 (2018).

[15] Y. Cao, V. Fatemi, S. Fang, K. Watanabe, T. Taniguchi, E. Kaxiras, and P. Jarillo-Herrero, Unconventional superconductivity in magic-angle graphene superlattices, Nature (London) **556**, 43 (2018).

[16] P. Rivera, J. R. Schaibley, A. M. Jones, J. S. Ross, S. Wu, G. Aivazian, P. Klement, K. Seyler, G. Clark, N. J. Ghimire *et al.*, Observation of long-lived interlayer excitons in monolayer $MoSe_2 - WSe_2$ heterostructures, Nat. Commun. **6**, 6242 (2015).

[17] K. Tran, G. Moody, F. Wu, X. Lu, J. Choi, K. Kim, A. Rai, D. A. Sanchez, J. Quan, A. Singh *et al.*, Evidence for moiré excitons in van der Waals heterostructures, Nature (London) **567**, 71 (2019).

[18] J. Xia, J. Yan, Z. Wang, Y. He, Y. Gong, W. Chen, T. C. Sum, Z. Liu, P. M. Ajayan, and Z. Shen, Strong coupling and pressure engineering in $WSe_2 - MoSe_2$ heterobilayers, Nat. Phys. **17**, 92 (2020).

[19] C. H. Jin, J. Kim, J. Suh, Z. W. Shi, B. Chen, X. Fan, M. Kam, K. Watanabe, T. Taniguchi, S. Tongay *et al.*, Interlayer electron-phonon coupling in WSe_2/hBN heterostructures, Nat. Phys. **13**, 127 (2017).

[20] C. M. Chow, H. Y. Yu, A. M. Jones, J. Q. Yan, D. G. Mandrus, T. Taniguchi, K. Watanabe, W. Yao, and X. D. Xu, Unusual exciton-phonon interactions at van der Waals engineered interfaces, Nano Lett. **17**, 1194 (2017).

[21] L. J. Du, Y. C. Zhao, Z. Y. Jia, M. Z. Liao, Q. Q. Wang, X. D. Guo, Z. W. Shi, R. Yang, K. Watanabe, T. Taniguchi *et al.*, Strong and tunable interlayer coupling of infrared-active phonons to excitons in van der Waals heterostructures, Phys. Rev. B **99**, 205410 (2019).

[22] Y. F. Li, X. W. Zhang, J. H. Wang, X. L. Ma, J. A. Shi, X. D. Guo, Y. G. Zuo, R. J. Li, H. Hong, N. Li *et al.*, Engineering interlayer electron-phonon coupling in WS_2/BN heterostructures, Nano Lett. **22**, 2725 (2022).

[23] L. Shi, P. Rohringer, K. Suenaga, Y. Niimi, J. Kotakoski, J. C. Meyer, H. Peterlik, M. Wanko, S. Cahangirov, A. Rubio *et al.*, Confined linear carbon chains as a route to bulk carbyne, Nat. Mater. **15**, 634 (2016).

[24] J. K. Qin, P. Y. Liao, M. Si, S. Gao, G. Qiu, J. Jian, Q. Wang, S. Q. Zhang, S. Huang, A. Charnas *et al.*, Raman response and transport properties of tellurium atomic chains encapsulated in nanotubes, Nat. Electron. **3**, 141 (2020).

[25] Z. K. Tang, L. Y. Zhang, N. Wang, X. X. Zhang, G. H. Wen, G. D. Li, J. N. Wang, C. T. Chan, and P. Sheng, Superconductivity in 4 angstrom single-walled carbon nanotubes, Science **292**, 2462 (2001).

[26] E. Bourgeois, M. V. Fernandez-Serra, and X. Blase, Radial breathing mode in silicon nanowires: An *ab initio* study, Phys. Rev. B **81**, 193410 (2010).

[27] E. Ghavanloo, S. A. Fazelzadeh, and H. Rafii-Tabar, Analysis of radial breathing-mode of nanostructures with various morphologies: A critical review, Int. Mater. Rev. **60**, 312 (2015).

[28] J. Zhou and J. Dong, Vibrational property and Raman spectrum of carbon nanoribbon, Appl. Phys. Lett. **91**, 173108 (2007).

[29] Y. Teng, Y. Zhang, X. Xie, J. Yao, Z. Zhang, L. Geng, P. Zhao, C. Yang, W. Gong, X. Wang *et al.*, Interfacial electron transfer in PbI_2 @single-walled carbon nanotube van der Waals heterostructures for high-stability self-powered photodetectors, J. Am. Chem. Soc. **146**, 6231 (2024).

[30] S. Liu, Y. Teng, Z. Zhang, J. Lai, Z. Hu, W. Zhang, W. Zhang, J. Zhu, X. Wang, Y. Li *et al.*, Interlayer charge transfer induced electrical behavior transition in 1D AgI@sSWCNT van der Waals heterostructures, Nano Lett. **24**, 741 (2024).

[31] Y. Lee, Y. W. Choi, K. Lee, C. Song, P. Ercius, M. L. Cohen, K. Kim, and A. Zettl, Tuning the sharing modes and composition in a tetrahedral GeX_2 (X = S, Se) system via one-dimensional confinement, ACS Nano **17**, 8734 (2023).

[32] T. Takenobu, T. Takano, M. Shiraishi, Y. Murakami, M. Ata, H. Kataura, Y. Achiba, and Y. Iwasa, Stable and controlled amphoteric doping by encapsulation of organic molecules inside carbon nanotubes, Nat. Mater. **2**, 683 (2003).

[33] X. Fan, E. C. Dickey, P. C. Eklund, K. A. Williams, L. Grigorian, R. Buczko, S. T. Pantelides, and S. J. Pennycook, Atomic arrangement of iodine atoms inside single-walled carbon nanotubes, Phys. Rev. Lett. **84**, 4621 (2000).

[34] H. P. Komsa, R. Senga, K. Suenaga, and A. V. Krasheninnikov, Structural distortions and charge density waves in iodine chains encapsulated inside carbon nanotubes, Nano Lett. **17**, 3694 (2017).

[35] M. Hart, E. R. White, J. Chen, C. M. McGilvery, C. J. Pickard, A. Michaelides, A. Sella, M. S. P. Shaffer, and C. G. Salzmann, Encapsulation and polymerization of white phosphorus inside single-wall carbon nanotubes, Angew. Chem. Int. Ed. **56**, 8144 (2017).

[36] J. Y. Zhang, C. C. Fu, S. X. Song, H. C. Du, D. Zhao, H. Y. Huang, L. H. Zhang, J. Guan, Y. F. Zhang, X. L. Zhao *et al.*, Changing the phosphorus allotrope from a square columnar structure to a planar zigzag nanoribbon by increasing the diameter of carbon nanotube nanoreactors, Nano Lett. **20**, 1280 (2020).

[37] E. Gaufres, N. Y. W. Tang, F. Lapointe, J. Cabana, M. A. Nadon, N. Cottenye, F. Raymond, T. Szkopek, and R. Martel, Giant Raman scattering from J-aggregated dyes inside carbon nanotubes for multispectral imaging, Nat. Photonics **8**, 73 (2014).

[38] G. H. Li, C. Y. Fu, M. B. Oviedo, M. G. Chen, X. J. Tian, E. Bekyarova, M. E. Itkis, B. M. Wong, J. C. Guo, and R. C. Haddon, Giant Raman response to the encapsulation of sulfur in narrow diameter single-walled carbon nanotubes, J. Am. Chem. Soc. **138**, 40 (2016).

[39] N. F. Andrade, A. L. Aguiar, Y. A. Kim, M. Endo, P. T. C. Freire, G. Brunetto, D. S. Galvao, M. S. Dresselhaus, and A. G. Souza, Linear carbon chains under high-pressure conditions, J. Phys. Chem. C **119**, 10669 (2015).

[40] W. Q. Neves, R. S. Alencar, R. S. Ferreira, A. C. Torres-Dias, N. F. Andrade, A. San-Miguel, Y. A. Kim, M. Endo, D. W. Kim, H. Muramatsu *et al.*, Effects of pressure on the structural and electronic properties of linear carbon chains encapsulated in double wall carbon nanotubes, Carbon **133**, 446 (2018).

[41] K. Sharma, N. L. Costa, Y. A. Kim, H. Muramatsu, N. M. B. Neto, L. G. P. Martins, J. Kong, A. R. Paschoal, and P. T. Araujo, Anharmonicity and universal response of linear carbon chain mechanical properties under hydrostatic pressure, Phys. Rev. Lett. **125**, 105501 (2020).

[42] E. L. Gao, K. Zhou, L. Shi, and Z. P. Xu, Comment on "Anharmonicity and universal response of linear carbon chain mechanical properties under hydrostatic pressure", Phys. Rev. Lett. **128**, 219601 (2022).

[43] H. Kuzmany, L. Shi, M. Martinati, S. Cambre, W. Wenseleers, J. Kurti, J. Koltai, G. Kukucska, K. C. Cao, U. Kaiser *et al.*, Well-defined sub-nanometer graphene ribbons synthesized inside carbon nanotubes, Carbon **171**, 221 (2021).

[44] See Supplemental Material at http://link.aps.org/supplemental/10.1103/PhysRevB.109.195413 for experimental method and sample description; calculation method; RBLMs of two kinds of AGNRs and full Raman spectrum of 6 AGNRs@mSWNT; Raman spectra of SWNTs; G band evolution of SWNT@6 AGNRs under pressure; Raman linewidths evolution of RBLMs of AGNRs and frequency shift evolution of left peak of 7 AGNRs under pressure; charge differential density for (18,0)SWNT@6 AGNRs and Na@6 AGNRs; deformation potential curves; the pressure evolution of the CH-ipb modes of 6 AGNRs; and which includes Refs. [45–48].

[45] S. Smidstrup, D. Stradi, J. Wellendorff, P. A. Khomyakov, U. G. Vej-Hansen, M. E. Lee, T. Ghosh, E. Jonsson, H. Jonsson, and K. Stokbro, First-principles Green's-function method for surface calculations: A pseudopotential localized basis set approach, Phys. Rev. B **96**, 195309 (2017).

[46] R. F. Bader, Atoms in molecules, Acc. Chem. Res. **18**, 9 (1985).

[47] G. Kresse and J. Furthmüller, Efficient iterative schemes for *ab initio* total-energy calculations using a plane-wave basis set, Phys. Rev. B **54**, 11169 (1996).

[48] T. Lu and F. W. Chen, Multiwfn: A multifunctional wavefunction analyzer, J. Comput. Chem. **33**, 580 (2012).

[49] J. M. Cai, C. A. Pignedoli, L. Talirz, P. Ruffieux, H. Sode, L. B. Liang, V. Meunier, R. Berger, R. J. Li, X. L. Feng *et al.*, Graphene nanoribbon heterojunctions, Nat. Nanotechnol. **9**, 896 (2014).

[50] Y. C. Lin, Z. Mutlu, G. B. Barin, Y. J. Hong, J. P. Llinas, A. Narita, H. Singh, K. Muellen, P. Ruffieux, R. Fasel *et al.*, Scaling and statistics of bottom-up synthesized armchair graphene nanoribbon transistors, Carbon **205**, 519 (2023).

[51] C. M. Hessel, J. W. Wei, D. Reid, H. Fujii, M. C. Downer, and B. A. Korgel, Raman spectroscopy of oxide-embedded and ligand-stabilized silicon nanocrystals, J. Phys. Chem. Lett. **3**, 1089 (2012).

[52] D. M. Sagar, J. M. Atkin, P. K. B. Palomaki, N. R. Neale, J. L. Blackburn, J. C. Johnson, A. J. Nozik, M. B. Raschke, and M. C. Beard, Quantum confined-electron phonon interaction in silicon nanocrystals, Nano Lett. **15**, 1511 (2015).

[53] U. Fano, Effects of configuration interaction on intensities and phase shifts, Phys. Rev. **124**, 1866 (1961).

[54] A. E. Miroshnichenko, S. Flach, and Y. S. Kivshar, Fano resonances in nanoscale structures, Rev. Mod. Phys. **82**, 2257 (2010).

[55] M. F. Limonov, M. V. Rybin, A. N. Poddubny, and Y. S. Kivshar, Fano resonances in photonics, Nat. Photonics **11**, 543 (2017).

[56] R. S. Wang, D. Peng, J. W. Hu, L. N. Zong, and X. J. Chen, Orientational ordering and electron-phonon interaction in K_3C_{60} superconductor, Carbon **195**, 1 (2022).

[57] H. Farhat, S. Berciaud, M. Kalbac, R. Saito, T. F. Heinz, M. S. Dresselhaus, and J. Kong, Observation of electronic Raman scattering in metallic carbon nanotubes, Phys. Rev. Lett. **107**, 157401 (2011).

[58] E. H. Hasdeo, A. R. T. Nugraha, K. Sato, M. S. Dresselhaus, and R. Saito, Electronic Raman scattering and the Fano resonance in metallic carbon nanotubes, Phys. Rev. B **88**, 115107 (2013).

[59] K. Y. Zhang, T. Wang, X. Q. Pang, F. Han, S. L. Shang, N. T. Hung, Z. K. Liu, M. D. Li, R. Saito, and S. X. Huang, Anisotropic Fano resonance in the Weyl semimetal candidate LaAlSi, Phys. Rev. B **102**, 235162 (2020).

[60] D. Q. Zhang, J. Yang, E. H. Hasdeo, C. Liu, K. H. Liu, R. Saito, and Y. Li, Multiple electronic Raman scatterings in a single metallic carbon nanotube, Phys. Rev. B **93**, 245428 (2016).

[61] H. Kataura, Y. Kumazawa, Y. Maniwa, I. Umezu, S. Suzuki, Y. Ohtsuka, and Y. Achiba, Optical properties of single-wall carbon nanotubes, Synth. Met. **103**, 2555 (1999).

[62] L. G. Moura, L. M. Malard, M. A. Carneiro, P. Venezuela, R. B. Capaz, D. Nishide, Y. Achiba, H. Shinohara, and M. A. Pimenta, Charge transfer and screening effects in polyynes encapsulated inside single-wall carbon nanotubes, Phys. Rev. B **80**, 161401(R) (2009).

[63] J. Gao, P. Blondeau, P. Salice, E. Menna, B. Bartova, C. Hebert, J. Leschner, U. Kaiser, M. Milko, C. Ambrosch-Draxl *et al.*, Electronic interactions between "pea" and "pod": The case of oligothiophenes encapsulated in carbon nanotubes, Small **7**, 1807 (2011).

[64] D. Q. Zhang, J. Yang, M. H. Li, and Y. Li, (n, m) assignments of metallic single-walled carbon nanotubes by Raman spectroscopy: The importance of electronic Raman scattering, ACS Nano **10**, 10789 (2016).

[65] Y. Hu, S. Chen, X. Cong, S. Sun, J. B. Wu, D. Zhang, F. Yang, J. Yang, P. H. Tan, and Y. Li, Electronic Raman scattering in suspended semiconducting carbon nanotube, J. Phys. Chem. Lett. **11**, 10497 (2020).

[66] M. G. Yao, Z. G. Wang, B. B. Liu, Y. G. Zou, S. D. Yu, W. Lin, Y. Y. Hou, S. F. Pan, M. X. Jin, B. Zou *et al.*, Raman signature to identify the structural transition of single-wall carbon nanotubes under high pressure, Phys. Rev. B **78**, 205411 (2008).

[67] A. San-Miguel, Nanomaterials under high-pressure, Chem. Soc. Rev. **35**, 876 (2006).

[68] B. Sundqvist, Carbon under pressure, Phys. Rep. **909**, 1 (2021).

[69] X. Li, T. Y. Zhang, and Y. J. Su, Periodically modulated size-dependent elastic properties of armchair graphene nanoribbons, Nano Lett. **15**, 4883 (2015).

[70] J. Bardeen and W. Shockley, Deformation potentials and mobilities in non-polar crystals, Phys. Rev. **80**, 72 (1950).

[71] W. A. Harrison, Scattering of electrons by lattice vibrations in nonpolar crystals, Phys. Rev. **104**, 1281 (1956).

[72] F. S. Khan and P. B. Allen, Deformation potentials and electron-phonon scattering: Two new theorems, Phys. Rev. B **29**, 3341 (1984).

[73] A. Chernikov, V. Bornwasser, M. Koch, S. Chatterjee, C. N. Böttge, T. Feldtmann, M. Kira, S. W. Koch, T. Wassner, S. Lautenschläger *et al.*, Phonon-assisted luminescence of polar semiconductors: Fröhlich coupling versus deformation-potential scattering, Phys. Rev. B **85**, 035201 (2012).

[74] F. Murphy-Armando, G. Fagas, and J. C. Greer, Deformation potentials and electron-phonon coupling in silicon nanowires, Nano Lett. **10**, 869 (2010).

[75] N. Yazdani, M. I. Bodnarchuk, F. Bertolotti, N. Masciocchi, I. Fureraj, B. Guzelturk, B. L. Cotts, M. Zajac, G. Rainò, M. Jansen *et al.*, Coupling to octahedral tilts in halide perovskite nanocrystals induces phonon-mediated attractive interactions between excitons, Nat. Phys. **20**, 47 (2023).

[76] J. Wiktor and A. Pasquarello, Absolute deformation potentials of two-dimensional materials, Phys. Rev. B **94**, 245411 (2016).

[77] T. Jentzsch, H. J. Juepner, K. W. Brzezinka, and A. Lau, Efficiency of optical second harmonic generation from pentacene films of different morphology and structure, Thin. Solid. Films **315**, 273 (1998).

[78] R. He, I. Dujovne, L. W. Chen, Q. Miao, C. F. Hirjibehedin, A. Pinczuk, C. Nuckolls, C. Kloc, and A. Ron, Resonant Raman scattering in nanoscale pentacene films, Appl. Phys. Lett. **84**, 987 (2004).

[79] M. Cazayous, A. Sacuto, G. Horowitz, P. Lang, A. Zimmers, and R. P. S. M. Lobo, Iodine insertion in pentacene thin films investigated by infrared and Raman spectroscopy, Phys. Rev. B **70**, 081309(R) (2004).

[80] H. L. Cheng, W. Y. Chou, C. W. Kuo, F. C. Tang, and Y. W. Wang, Electric field-induced structural changes in pentacene-based organic thin-film transistors studied by *in situ* micro-Raman spectroscopy, Appl. Phys. Lett. **88**, 161918 (2006).

[81] H. L. Cheng, W. Y. Chou, C. W. Kuo, Y. W. Wang, Y. S. Mai, F. C. Tang, and S. W. Chu, Influence of electric field on microstructures of pentacene thin films in field-effect transistors, Adv. Funct. Mater. **18**, 285 (2008).

[82] T. Breuer, M. A. Celik, P. Jakob, R. Tonner, and G. Witte, Vibrational Davydov splittings and collective mode polarizations in oriented organic semiconductor crystals, J. Phys. Chem. C **116**, 14491 (2012).

[83] W. H. Butler and R. K. Williams, Electron-phonon interaction and lattice thermal conductivity, Phys. Rev. B **18**, 6483 (1978).

[84] J. Neve, B. Sundqvist, and Ö. Rapp, Electron band structure, resistivity, and the electron-phonon interaction for niobium under pressure, Phys. Rev. B **28**, 629 (1983).

[85] G. S. N. Eliel, M. V. O. Moutinho, A. C. Gadelha, A. Righi, L. C. Campos, H. B. Ribeiro, P. W. Chiu, K. Watanabe, T. Taniguchi, P. Puech *et al.*, Intralayer and interlayer electron-phonon interactions in twisted graphene heterostructures, Nat. Commun. **9**, 1221 (2018).